

LIMIT ANALYSIS PROBLEMS INCLUDING FRICTIONAL CONTACT

Liliana Naccarato, liliana@mecsol.ufrj.br

Lavinia Alves Borges, lavinia@mecanica.ufrj.br

Solid Mechanics Laboratory

Universidade Federal do Rio de Janeiro, COPPE/PEM

PO Box 68503, Zip code 21945-970, Rio de Janeiro, RJ, Brasil

Abstract. *The main objective of this work is to propose a limit analysis procedure to study manufacturing problems in which the frictional conditions are crucial issues on the control of the process. The proposed methodology includes a variational description of the problem and a numerical model, based on finite element technic and optimization algorithms, in order to solve the discretized version of problem. Two important processes are considered in the analysis: the orthogonal cutting and the equal channel angular extrusion. In the first case the limit analysis approach can be a powerful tool to estimate the cut power and to localize the chip-tool contact interface for different friction conditions. The equal channel angular extrusion is one of the most used processes to produce nano-structured metallic materials. The ultrafine grain structure is obtained by the imposition of severe plastic deformation in the material without substantial changes in the external dimension of the specimen. By limit analysis the work pressure can be determined and the correlation between the microstructure of the material and the friction in material-matrix interface can be established. Furthermore, the influence of the inlet angle and the outlet channel in quality of the produced material can be studied.*

Keywords: *Limit Analysis, Frictional Contact, Orthogonal Cutting, Equal Channel Angular Extrusion.*

1. INTRODUCTION

The main objective of this work is to propose a limit analysis procedure to study manufacturing problems in which the frictional conditions are crucial issues on the control of the process. The proposed methodology includes a variational description of the problem and a numerical model, based on finite element method and optimization algorithms, in order to solve the discretized version of the problem.

Under the assumption of proportional loading, the limit analysis problem consists in finding a load factor α such that the body undergoes plastic collapse when subject to the reference loads F uniformly amplified by α . In turn, a system of loads produces plastic collapse if there exists a stress field in equilibrium with these loads, which is plastically admissible and related by the constitutive equations to a plastic strain rate field being kinematically admissible.

The limit analysis studies the body behavior in an incipient situation of plastic flow or plastic collapse. The plastic flow and plastic collapse concepts are essentially equivalents. But from physical point of view these concepts have very different meanings. The plastic collapse describes an incipient situation of developing large and undesirable deformations in a certain body configuration. The concept of plastic flow is applied to describing the steady-state process in which is desired to molding a solid by conveniently applied forces.

Two important processes are considered in the analysis: the orthogonal cutting and the equal channel angular extrusion.

Several models have been developed to describe the orthogonal cutting process; some have been fairly successful in describing the process, but none can be fully substantiated and definitely stated to be the correct solution. Thus, while none of the analysis can precisely predict conditions in a practical cutting situation, the analysis are worth examining because they can qualitatively explain phenomena observed and indicated the direction in which conditions should be changed to improve cutting performance. In the cutting process the limit analysis approach can be a powerful tool to estimate the cut power and to localize the chip-tool contact interface under different friction conditions.

The equal channel angular extrusion is one of the most used processes to produce nano-structured metallic materials (Segal, 2003). The ultra fine grain structure is obtained by the imposition of severe plastic deformation in the material without substantial changes in the external dimension of the specimen. By limit analysis the work pressure can be determined and the correlation between the micro-structure of the material and the friction in material-matrix interface can be established. Furthermore, the influence of the inlet angle and the outlet channel in quality of the produced material can be studied.

2. CONTACT MECHANICS

In this section it is presented the kinematics conditions and the equilibrium to a body \mathcal{B} with regular boundary Γ , submitted to volume load b and at the boundary Γ_τ to the surface loads τ . At the boundary Γ_v the velocities are imposed null and at the boundary Γ_c are imposed unilateral contact conditions with friction ($\Gamma = \Gamma_v \cup \Gamma_\tau \cup \Gamma_c$ and $\Gamma_v \cap \Gamma_\tau \cap \Gamma_c = \emptyset$).

In the initial configuration \mathcal{B}_0 there is a face of the body in full contact with a motionless planar rigid surface. The contact surface is defined by an orthogonal unitary vector \mathbf{n} directed outwards from the body throughout Γ_c . On the rigid surface the vector \mathbf{n} forms an orthogonal local basis with the unit tangent vector \mathbf{t} (Figure 1).

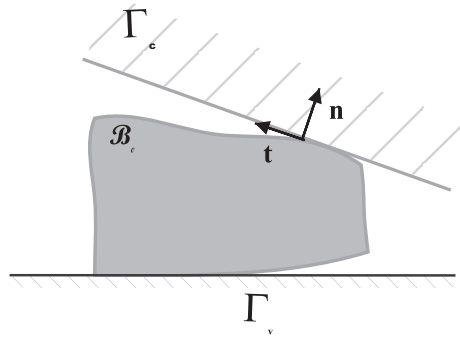


Figure 1. Geometric characteristics.

In this context, the field of kinematically admissible velocities is defined by

$$V = \{ \mathbf{v} \in \mathbb{R}^3 \mid v_n \leq 0 \quad x \in \Gamma_c \text{ and } \mathbf{v} = 0, \quad x \in \Gamma_v \}. \quad (1)$$

As result of the external loading, a contact force distribution \mathbf{r} is developed on the contact surface Γ_c in such way that

$$\mathbf{r} = \boldsymbol{\sigma} \mathbf{n}, \quad (2)$$

where $\boldsymbol{\sigma}$ is the Cauchy tensor. The traction vector \mathbf{r} can be decomposed as

$$\mathbf{r} = r_n \mathbf{n} + \mathbf{r}_t, \quad (3)$$

where $r_n \mathbf{n}$ and \mathbf{r}_t are the normal and tangential components, respectively. In turn, the dual velocity vector can be decomposed in the tangential and normal component, that is

$$\mathbf{v} = v_n \mathbf{n} + \mathbf{v}_t, \quad (4)$$

where $v_n = \mathbf{v} \cdot \mathbf{n}$ is the normal component \mathbf{v} , and $\mathbf{v}_t = \mathbf{v} - v_n \mathbf{n}$ the tangential component.

The contact body region is initially in contact with the surface and is allowed to separate but not to cross the rigid surface. If body must remain in contact with the rigid surface than $v_n = 0$ and $r_n \leq 0$; or must separate, than $v_n < 0$ and $r_n = 0$. This rate unilateral contact law can be written as:

$$v_n \leq 0 \quad r_n \leq 0 \quad v_n r_n = 0, \quad \text{on } \Gamma_c \quad (5)$$

The rate formulation of Signorini conditions Eq. (5), also known as *complementarity conditions* (Kikuchi and Oden, 1988), can be combined with the sliding rule to derive the full friction contact law to the contact region, given next.

2.1 Coulomb Friction Model

Let f a function defined as:

$$f(\mathbf{r}_t, r_n) = \|\mathbf{r}_t\| - \mu |r_n|, \quad (6)$$

where $\|\mathbf{r}_t\| = \sqrt{\mathbf{r}_t \cdot \mathbf{r}_t}$ and μ is the coefficient of friction.

The gradient of the function f can be written as

$$\nabla f = \frac{\mathbf{r}_t}{\|\mathbf{r}_t\|} + \mu \mathbf{n}. \quad (7)$$

The convex set K_μ , containing all the allowed contact forces \mathbf{r} , is defined by (De Saxce and Bousshine, 1998)

$$K_\mu = \{ \mathbf{r} \in \mathbb{R}^3 \mid f(\mathbf{r}_t, r_n) \leq 0 \}. \quad (8)$$

The symbols oK_μ and ∂K_μ are adopted to denote the interior and the boundary of K_μ , respectively.

2.2 The Frictional Contact Law

In the non-associated sliding law, defined in the sequel, the sliding direction is given by the gradient of the friction cone and its magnitude by the multiplier $\dot{\lambda}$, or equivalently

$$v_n = 0 \quad (9)$$

$$-\mathbf{v}_t = \dot{\lambda} \nabla_{\mathbf{r}_t} f = \dot{\lambda} \frac{\mathbf{r}_t}{\|\mathbf{r}_t\|}, \quad \dot{\lambda} = \|\mathbf{v}_t\|; \quad (10)$$

where the multiplier $\dot{\lambda}$ are required to satisfy the complementarity relations:

$$f(\mathbf{r}_t, r_n) = \|\mathbf{r}_t\| - \mu |r_n| \leq 0; \quad \dot{\lambda} \geq 0; \quad \dot{\lambda} f(\mathbf{r}_t, r_n) = 0. \quad (11)$$

The inverse relation of (9-10), to $v_n = 0$, is given by:

$$r_n \leq 0 \quad (12)$$

$$\mathbf{r}_t = |r_n| \mu \frac{-\mathbf{v}_t}{\|\mathbf{v}_t\|}. \quad (13)$$

The friction law (9-10) and its inverse form (12-13) define a dissipative non-associate law since the sliding direction is not normal to the Coulomb Cone, but co-linear to the frictional tangential force. The full friction contact law to the contact region, summarized in the **Box1** and **Box2**, is derived by the combination of these laws with the Signorini conditions (5).

Box 1 Sliding Law

if $r_n = 0$ then	\triangleright <i>Non contact</i>
$v_n \leq 0$	
else if $\mathbf{r} \in oK_\mu$ then	\triangleright <i>Non sliding</i>
$v_n = 0$ e $\mathbf{v}_t = 0$	
else ($\mathbf{r} \in \partial K_\mu$ e $r_n < 0$)	\triangleright <i>Sliding</i>
$v_n = 0$ and $\exists \dot{\lambda}$ such that $-\mathbf{v}_t = \dot{\lambda} \frac{\mathbf{r}_t}{\ \mathbf{r}_t\ }$	
end if	

Box 2 Inverse Sliding Law

if $v_n < 0$ then	\triangleright <i>Non Contact</i>
$r_n = 0$	
else if $\mathbf{v} = 0$ then	\triangleright <i>Non sliding</i>
$\mathbf{r} \in oK_\mu$	
else if $v_n = 0$ then	\triangleright <i>Sliding</i>
$r_n \leq 0$ and $\mathbf{r}_t = r_n \mu \frac{\mathbf{v}_t}{\ \mathbf{v}_t\ }$	
end if	

Equivalently, the model described above may be considered as an Implicit Standard Material Law by defining a generalized potential of dissipation that belongs to the class of bipotentials extensively studied by Géry de Saxcé and coworkers (De Saxcé and Feng, 1998, and De Saxcé and Bousshine, 1998). The bipotential described here, is given in (De Saxcé and Feng, 1998) by

$$b_c(-\mathbf{v}, \mathbf{r}) = \text{Ind}_{\mathbb{R}_+}(-v_n) + \text{Ind}_{K_\mu}(\mathbf{r}) + \mu |r_n| \|\mathbf{v}_t\|, \quad (14)$$

where \mathbb{R}_+ is the set of the positive and null real numbers and $\mathcal{I}_A(\cdot)$ denotes the indicator function of the set A . Then, the implicit law of unilateral contact with dry friction defined in the **Box 1** and **Box 2** can be represented by the following subdifferential inclusion (De Saxcé and Bousshine, 1998, Naccarato, 2006):

$$-\mathbf{v} \in \partial_{\mathbf{r}} b_c(-\mathbf{v}, \mathbf{r}) \Leftrightarrow \mathbf{r} \in \partial_{-\mathbf{v}} b_c(-\mathbf{v}, \mathbf{r}). \quad (15)$$

2.3 EQUILIBRIUM

For a compatible strain field, related to \mathbf{v} by $\mathbf{d} = \nabla^s \mathbf{v}$, the equilibrium conditions relating a stress field and a load system proportional to a prescribed $\mathbf{F} \in \mathbf{V}'$, is imposed by the principle of virtual power (Kikuchi, 1988):

$$\langle \boldsymbol{\sigma}, \nabla^s \mathbf{v}^* \rangle - \langle \mathbf{r}, \mathbf{v}^* \rangle_{\Gamma_c} = L(\mathbf{v}^*), \quad \forall \mathbf{v}^* \in V; \quad (16)$$

where the internal power associated is defined by $\langle \boldsymbol{\sigma}, \mathbf{d} \rangle = \int_{\mathcal{B}} \boldsymbol{\sigma} \cdot \mathbf{d} \, d\mathcal{B}$, the external power by $L(\mathbf{v}) = \int_{\mathcal{B}} \mathbf{b} \cdot \mathbf{v} \, d\mathcal{B} + \int_{\Gamma_t} \boldsymbol{\tau} \cdot \mathbf{v} \, d\Gamma_t$ and $\langle \mathbf{r}, \mathbf{v} \rangle_{\Gamma_c} = \int_{\Gamma_c} \mathbf{r}(\boldsymbol{\sigma}) \cdot \mathbf{v} \, d\Gamma_c$.

The b_c (14) is a bipotential. Therefore it is separately convex with respect to \mathbf{v} and \mathbf{r} and satisfies the following condition (Zouain et al., 2007, Naccarato, 2006, De Saxce and Feng, 1998, and De Saxce and Bousshine, 1998)

$$\mathbf{b}_c(-\mathbf{v}, \mathbf{r}) \geq - \langle \mathbf{r}, \mathbf{v} \rangle_{\Gamma_c} \quad \forall (\mathbf{v}, \mathbf{r}), \quad (17)$$

where $\mathbf{b}_c(\mathbf{v}, \mathbf{r}) = \int_{\Gamma_c} b_c(\mathbf{v}, \mathbf{r}) \, d\Gamma_c$.

By combining (17) and (16) ones is obtained

$$\langle \boldsymbol{\sigma}, \nabla^s \mathbf{v}^* \rangle + \mathbf{b}_c(-\mathbf{v}^*, \mathbf{r}) - L(\mathbf{v}^*) \geq 0, \quad \mathbf{v}^* \in V, \quad (18)$$

with \mathbf{v}, \mathbf{r} linked by the contact flow rule (15).

The inequality (18) can be written in a compact way as $\boldsymbol{\sigma} \in S_\alpha$, where S_α represents the set of all stress fields equilibrated with a fixed force system amplified by the load factor or collapse load $\alpha \in \mathbb{R}^+$, that is, the collapse load system is defined by $\alpha L(\mathbf{v})$.

3. CONSTITUTIVE RELATIONS FOR ELASTIC-IDEALLY PLASTIC MATERIALS

The stress field $\boldsymbol{\sigma}$ in an elastic-ideally plastic body \mathcal{B} is constrained to fulfill the plastic admissibility condition, i.e. it must belong to the set

$$P = \{ \boldsymbol{\sigma} \in W' \mid f(\boldsymbol{\sigma}) \leq 0 \in \mathcal{B} \}, \quad (19)$$

where f is a m -vector valued function describing the yield criterion. The inequality above is then understood as imposing that each component f_k , which is a regular convex function of $\boldsymbol{\sigma}$, is non-positive.

The stresses corresponding to a given plastic strain rate complies with the principle of maximum dissipation and can be written as: (Borges et al., 1996, and the references herein).

$$\boldsymbol{\sigma} \in \partial \mathcal{X}(D^p) \Leftrightarrow D^p \in C_p(\boldsymbol{\sigma}), \quad (20)$$

where $\mathcal{X}(D^p)$ is the dissipation function, defined as

$$\mathcal{X}(D^p) = \sup_{\boldsymbol{\sigma}^* \in P} \langle \boldsymbol{\sigma}^*, D^p \rangle. \quad (21)$$

The symbol $\partial \mathcal{X}(D^p)$ represents the subdifferential of the dissipation function and $C_p(\boldsymbol{\sigma})$ is the cone of normals to the plastic admissible set P at $\boldsymbol{\sigma}$.

At any point of \mathcal{B} , the Eq. (20) is equivalent to the normality rule $D^p = \nabla f(\boldsymbol{\sigma}) \dot{\lambda}$, where $\nabla f(\boldsymbol{\sigma})$ denotes the gradient of f , and $\dot{\lambda}$ is the \hat{m} -vector field of plastic multipliers. At any point of \mathcal{B} , the components of $\dot{\lambda}$ are related to each plastic mode in f by the complementarity condition $\dot{\lambda}_j \geq 0, f_j \leq 0$ and $f_j \cdot \dot{\lambda}_j = 0$ (Lubliner, 1990, Borges, 1996).

4. PLASTIC COLLAPSE

Limit Analysis consists of finding the load factor $\alpha > 0$ that amplifies a prescribed loading until the incipient plastic collapse is attained. The collapse load is equilibrated with a stress field associated, through the constitutive relation, to a compatible purely plastic strain rate. Briefly, the plastic collapse is characterized by the fields $(\boldsymbol{\sigma}, \mathbf{v}, D)$ that comply with the following system of equations and inequations (De Saxce and Bousshine, 1998, Naccarato, 2006):

$$D^p = \nabla^s \mathbf{v}, \quad \text{in } \Omega \quad \text{for } \mathbf{v} \in V \quad (22)$$

$$\langle \boldsymbol{\sigma}, \nabla^s \mathbf{v}^* \rangle + \mathbf{b}_c(-\mathbf{v}^*, \mathbf{r}) - \alpha L(\mathbf{v}^*) \geq 0, \quad \forall \mathbf{v}^* \in V \quad (23)$$

$$-\mathbf{v} \in \partial_r \mathbf{b}_c(-\mathbf{v}, \mathbf{r}) \Leftrightarrow \mathbf{r} \in \partial_{-\mathbf{v}} \mathbf{b}_c(-\mathbf{v}, \mathbf{r}) \quad (24)$$

$$\boldsymbol{\sigma} \in \partial \mathcal{X}(D^p) \Leftrightarrow D^p \in \partial \text{Ind}_P(\boldsymbol{\sigma}) \quad (25)$$

Purely static or kinematic optimization principles can also be proposed to describe the limit analysis problems in which no unilateral conditions or, at most, only frictionless unilateral conditions are prescribed. This optimization principles and a system defined as (22-25) are equivalents, so they furnish the same result. This is no true for the model herein presented. In fact, the limit analysis with frictional boundary condition can only be expressed by a bipotential, where the fields (σ, v, r) are coupled in an implicit relationship defined by the inclusion (24). Moreover, the equivalency between the proposed principle and the above system is not yet established, as well as the general conditions to guarantee the existence and unicity of the solution for plastic collapse problems (De Saxce and Bousshine, 1998c, Naccarato, 2006).

A finite element model for the system (22-25) and a Newton-like strategy for solving this discretion version is proposed by Naccarato (2006) and were adopted to solve the problems presented in the sequel.

5. NUMERICAL APPLICATIONS

In this section it is presented the study of two metal forming processes where the proposed model for limit analysis with friction can be effectively applied.

5.1 Orthogonal Cutting

An orthogonal metal cutting process is described by an Eulerian configuration representing the steady state motion of the workpiece relative to a stationary cutting tool. This geometrical model is defined on Fig. 2.

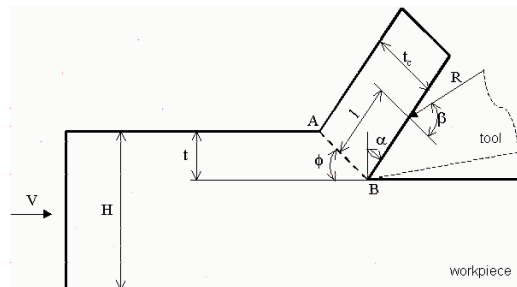


Figure 2. Orthogonal Cutting. Geometric characteristics

The model consists of a workpiece of thickness H moving toward a stationary tool at a constant speed V while a non-deformed chip thickness t is being cut away; in the same way, a deformed chip thickness t_c is machined. A layer of large shear deformation occurs along the plane AB (the shear plane) inclined at an angle ϕ (shear angle) to the horizontal line; α is the tool rake angle and β is the friction angle between the resultant force R and the normal to the rake face. The width of the chip is assumed to be large as compared with the cutting depth t and the chip thickness t_c . This assures the two dimensional plane strain model (Tyan and Yang, 1992).

Here the effects of strain rate and temperature are not considered, the tool is assumed rigid and the workpiece is modelled to be infinitely ductile. The last hypothesis is adequate with the continuous chip formation model adopted. The high strain rates that accompany the machining operation are said to raise the yield strength of the material and make it approximate the idealized plastic material (Johnson and Mellor, 1973). The Von Mises yield criterion behavior is assumed.

In spite of its technological importance and influence in the final processes behavior, the determination of the exact chip-tool contact region is a difficult task. Many authors (Tyan and Yang, 1992) adoptes the controlled contact model, that is, the tool-chip contact length l is previously settled. This strategy is efficient to the frictionless problems but not to the frictional ones that are here considered. Therefore, the proposed limit analysis procedure, in association with an adaptive mesh strategy, is projected to automatically identify, not only the chip-tool contact regions, but also, the shear region AB defined by the shear angle ϕ (Fig. 2).

In the present work the orthogonal cutting was simulated considering two different rake angle, the rake angles $\alpha = 20^\circ$ and $\alpha = 30^\circ$; the cutting depth is assumed $t = 0.3H$ and all other geometrical parameters were referred to this parameter. The Coulomb friction coefficient μ represents the lubrication condition, where $\mu = 0.0$ represents de perfect lubrication, or frictionless condition. A typical value to the Coulomb friction is $\mu = 0.6$.

In Fig. 3, it is presented the adaptative mesh and velocity field to $\alpha = 30^\circ$, with and without friction, where (a) presents the initial mesh and (b) the the obtained mesh after four adaptive mesh iterations. The velocity fields are shown in Fig. 3 (c) and (d).

The velocity distributions on the chip-tool interface is depicted in Fig. 4(a). The distribution of normal velocities shows the difference between the frictional contact region's length and frictionless ones. The contact region for the frictionless interface finishes at $l = 1$ while the frictional one this value is greater than 1.5. In the same figure, it can be observed that for the frictional case there is a region between $0 \leq l \leq 0.2$ where the tangential velocity is zero, indicating a adhesion

condition. The remained contact region presents contact with frictional sliding.

The evolution along the iterative process of the loads' amplifying factors, considering the reference loads equal to one, are shown in Fig. 4(b).

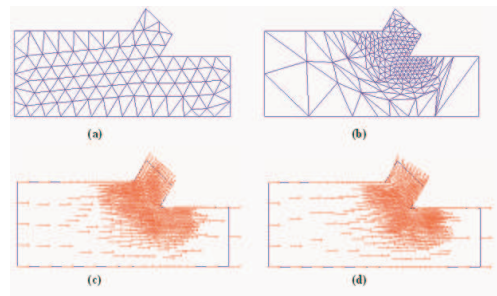


Figure 3. Orthogonal Cutting to $\alpha = 30^0$. (a) initial mesh (b) After four adaptive iterations . The velocity field to (c) $\mu = 0.6$ (d) $\mu = 0.0$.

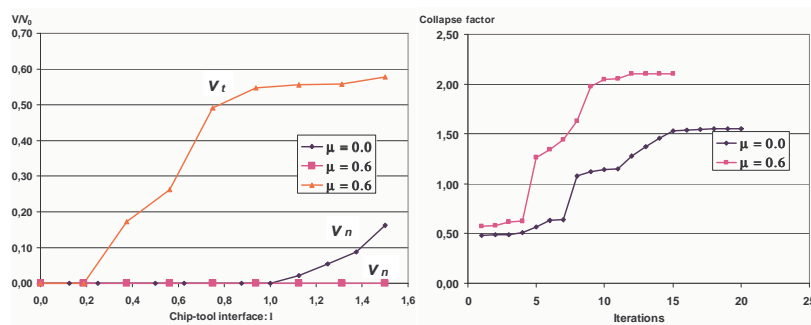


Figure 4. Orthogonal Cutting 30^0 . (a) Velocity components on the chip-tool interface. (b) Collapse factor.

Figure 5 presents the results comparing the normal reaction and the load factor to two different rake angles considered, and the Fig. 6 the plastic strain rate in the chip-tool interface to $\mu = 0.6$ and $\mu = 0.0$.

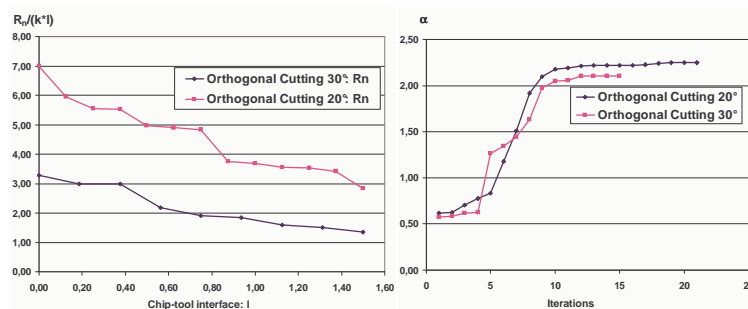


Figure 5. Orthogonal Cutting $30^0 \times 20^0$. (a) Normal reaction in the chip-tool interface; (b) Collapse factor.

5.2 Equal Channel Angular Extrusion

Nowadays, the equal channel angular extrusion - Fig. 7(a) is one of the most used processes to produce nano-structured metallic materials (Segal, 2003). The ultrafine grain structure is obtained by the imposition of severe plastic deformation in the material without substantial changes in the external dimension of the specimen. By limit analysis the work pressure can be determined and the correlation between the microstructure of the material and the friction in material-matrix interface can be established. Furthermore, the influence of the inlet angle and the outlet channel in quality of the produced material can be studied.

This process simulation was carried out by considering an extreme situation: extrusion channel of 90^0 and coefficient of friction $\mu = 1.0$, indicating a total adhesion of the material nearby the matrix's wall.

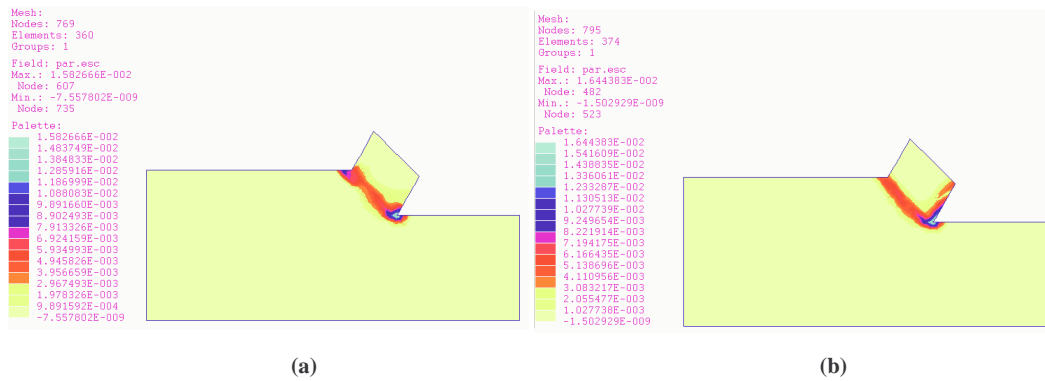


Figure 6. Orthogonal Cutting 30⁰: Plastic strain rate in the chip-tool interface to (a) $\mu = 0.6$ and to (b) $\mu = 0.0$.

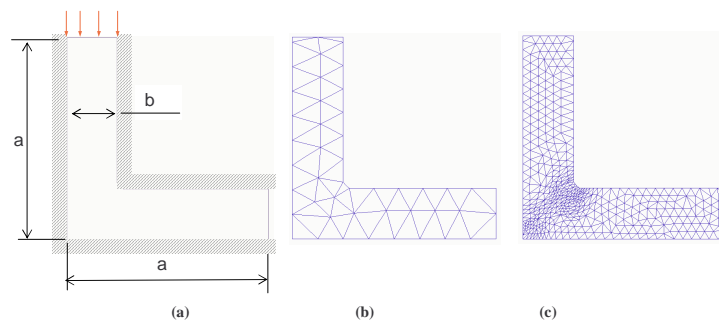


Figure 7. Extrusion channel of 90⁰: (a) geometry, loading and boundary conditions. Adaptive mesh: (b) initial mesh and (c) final mesh.

An important parameter is the plastic strain region localization. To this, an adaptive mesh procedure (Borges *et al*, 2001) was adopted. The initial considered and the final mesh adopted after the adaptive process are depicted in the Fig. 7 (b) and (c), respectively.

In Fig. 8, the obtained plastic strain distribution is presented. To the frictionless case - (a) - the concentration occurred at the region where the channel changes the flow direction. To the friction case - (b) - due to the extreme situation of adhesion ($\mu = 1.0$), the plastic strain concentration occurs on the outlet channel's walls.

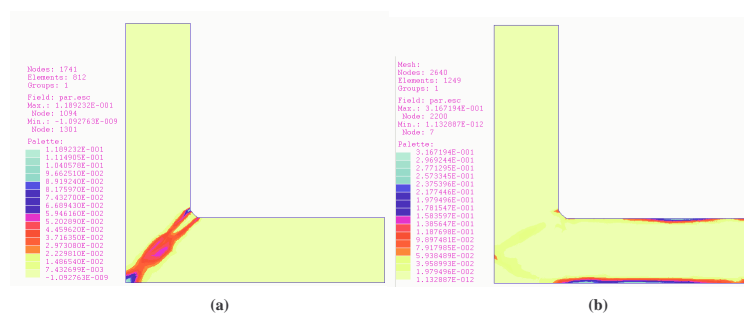


Figure 8. Extrusion channel of 90⁰. Plastic strain rate: (a) $\mu = 0.0$; (b) $\mu = 1.0$

It is important to observe on Fig. 9, the velocity's behavior near the region where the channel changes the flow direction. At this region, for the frictional case, the present simulation was able to identify the existence of a empty space in the matrix, named "death zone", previously cited by Segal (2003). The inclusion of the frictional condition was conclusive in order to capture this behavior, not observed for the frictionless cases.

The normal reaction distribution on the matrix-material interface, shown in the Fig. 9 (c) and (d), is another important parameter to be considered. It is important to note that to the friction case the normal reaction rise up substantially.

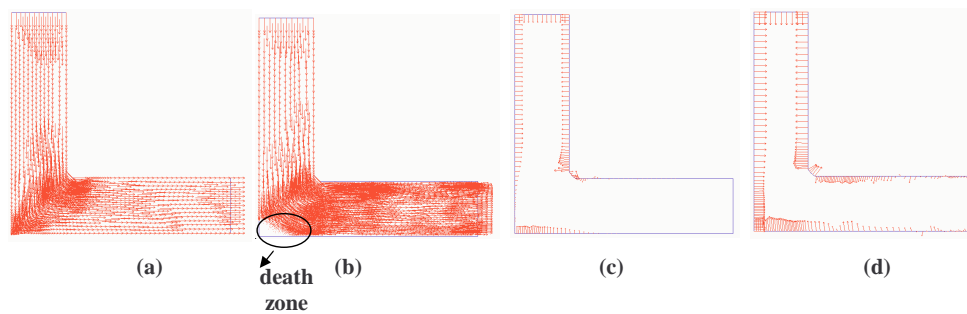


Figure 9. Extrusion channel of 90° . Velocity field: (a) $\mu = 0.0$; (b) $\mu = 1.0$. Normal reaction distribution: (c) $\mu = 0.0$; (d) $\mu = 1.0$.

6. CONCLUSIONS

A limit analysis variational approach was presented to study manufacturing problems in which the frictional condition is an important parameter to define the process response. The proposed strategy includes finite elements models, adaptive strategy and optimization algorithms. In spite of are a lot of open questions concerning the existence of solution for limit analysis frictional problems, the present methodology was efficient to answer important questions about the Orthogonal Cutting and the Equal Channel Angular Extrusion procedure, showing up the fundamental characteristics of the processes.

7. ACKNOWLEDGEMENTS

The authors would like to acknowledge the support of this research by their own institutions and by CAPES.

8. REFERENCES

- Borges, L., Zouain, N., and Huespe, A., 1996, "A nonlinear optimization procedure for limit analysis.", *European Journal of Mechanics A/Solids*, 15:487–512.
- Borges, L., Zouain, N., Alves, C. G., and Feijóo, R., 2001. "An adaptive approach to limit analysis.", *International Journal of Solids e Structures*, 38:1707–1720.
- Bousshine, L., Chaaba, A., and de Saxce, G. ,2002,. "Plastic limit load of plane frames with frictional contact supports", *International Journal of Mechanical Sciences*, 44:2189–2216.
- De Saxce, G. and Bousshine, L. (1998). "Limit analysis theorems for implicit steard materials: Application to the unilateral contact with dry friction e the non-associated flow rules in solids e rocks.", *International Journal of Mechanical Sciences*, 40(4):387–398.
- De Saxce, G. and Feng, Z.-Q. (1998). "The bipotential method: A construtive approach to design the complete contact law with friction e improved numerical algorithms." *Mathematical Comput. Modelling*, 26(4):225–245.
- Johnson, W. and Mellor, P.B., 1973 "Engineering Plasticity", Van Nostre Reinhold Company.
- Kikuchi, N. and Oden, J., 1988 "Contact Problems in Elasticity: A study of Variational Inequalities and Finite Element Methods", SIAM.
- Lubliner, J., 1990, "Plasticity theory", Mcmillan Publishing Company, New York.
- Hjjaja, M., Feng, Z.-Q., Saxce, G., Mroz, Z., 2004, "On the modelling of complexan isotropic frictional contact-laws", *International*
- Naccarato, L., 2006. "Análise Limite com Condições de Contorno Unilaterais.", Tese de Doutorado, COPPE/PEM-UFRJ (*in portuguese*).
- Segal, V., 2003, "Slip line solutions, deformation mode e loading history during equal channel angular extrusion.", *Materials Science e Engineering*, A345:36–46.
- Tyan, T. and Yang, W. ,1992, "Analysis of orthogonal metal cutting process.", *Int. J. Solids Structures*, 34:365–389. *Journal of Engineering Science* 42:1013–1034.

9. Responsibility notice

The authors are the only responsible for the printed material included in this paper.